Environmental Science & Technology

pubs.acs.org/est

Article

Comparison of Phase States of $PM_{2.5}$ over Megacities, Seoul and Beijing, and Their Implications on Particle Size Distribution

Mijung Song,* Rani Jeong, Daeun Kim, Yanting Qiu, Xiangxinyue Meng, Zhijun Wu, Andreas Zuend, Yoonkyeong Ha, Changhyuk Kim, Haeri Kim, Sanjit Gaikwad, Kyoung-Soon Jang, Ji Yi Lee, and Joonyoung Ahn

Cite This: *Environ. Sci. Technol.* 2022, 56, 17581−17590

Read Online

ACCESS | Metrics & More | Article Recommendations | Supporting Information

ABSTRACT: Although the particle phase state is an important property, there is scant information on it, especially, for real-world aerosols. To explore the phase state of fine mode aerosols ($PM_{2.5}$) in two megacities, Seoul and Beijing, we collected $PM_{2.5}$ filter samples daily from Dec 2020 to Jan 2021. Using optical microscopy combined with the poke-and-flow technique, the phase states of the bulk of $PM_{2.5}$ as a function of relative humidity (RH) were determined and compared to the ambient RH ranges in the two cities. $PM_{2.5}$ was found to be liquid to semisolid in Seoul but mostly semisolid to solid in Beijing. The liquid state was dominant on polluted days, while a semisolid state was dominant on clean days in Seoul. These findings can be explained by the aerosol liquid water content related to the chemical compositions of the aerosols at ambient RH; the water content of $PM_{2.5}$ was much higher in Seoul than in Beijing. Furthermore, the overall phase states of $PM_{2.5}$ observed in Seoul and Beijing were interrelated with the particle size distribution. The results of this study aid in a better understanding of the fundamental physical properties of aerosols and in examining how these are linked to $PM_{2.5}$ in polluted urban atmospheres.

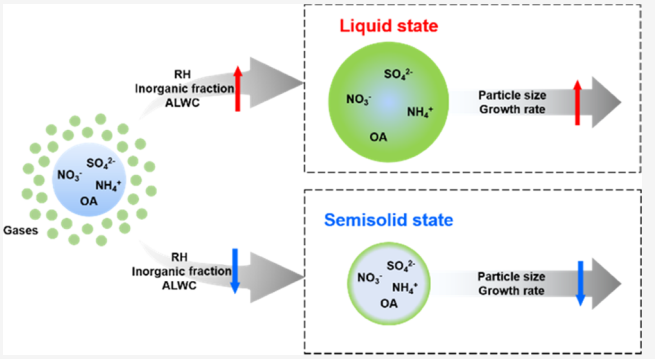

KEYWORDS: *phase state, morphology, $PM_{2.5}$, aerosol liquid water content, size distribution, megacities*

1. INTRODUCTION

Rapid economic and industrial development in Asia over recent decades has resulted in serious aerosol pollution. Fine particulate matter consisting of effective diameters less than 2.5 micrometers ($PM_{2.5}$) plays an important role in determining the air quality and affects climate change and human health.[1−3] These effects are influenced by various physicochemical properties of $PM_{2.5}$, such as the phase state (often reported via the viscosity), morphology, hygroscopicity, size distribution, and chemical composition.[4] Moreover, the liquefaction and solidification of $PM_{2.5}$ are dependent on the aerosol liquid water content (ALWC), which can also be related to the aerosol phase states (i.e., liquid, semisolid, or solid).[5,6] The interrelationship between chemical composition, phase state, and the ALWC might be critical in an accurate prediction of aerosol pollution and its links to regional climate.

Most recent studies on the phase states of aerosol particles have been conducted using laboratory experiments on different types of secondary organic aerosols (SOAs), mixtures of SOAs, and secondary inorganic aerosols (SIAs).[7−13] Experiments using lab-made atmospherically relevant aerosol particles revealed that aerosol particles exist not only in the liquid state, as had been conventionally used in kinetic models, but also in semisolid and/or solid states depending on aerosol composition, relative humidity (RH), and temperature.[11,13,14] Aerosol phase states and behaviors are key parameters for enabling more accurate predictions of mass concentration, growth rate, and heterogeneous reactivity of aerosols.[15−19] For example, in liquid-state aerosol particles, reactions with accommodated gas molecules can occur in the bulk of the particles, and therefore, particle size can be increased relatively rapidly with a higher mass concentration of condensable species. However, in solid-state aerosol particles, reactions with molecules of the gas-phase origin are mostly confined to the surface of the particles, resulting in slower growth and smaller sizes of particles compared to the case of liquid aerosol particles.[19]

Received: September 1, 2022
Revised: November 20, 2022
Accepted: November 21, 2022
Published: December 2, 2022

Table 1. Summary of Daily Average Mass Concentration, Oxygen-to-Carbon Ratio (O:C) of $PM_{2.5}$, and Ambient Relative Humidity (RH) in Seoul and Beijing[a]

year	date (MM/dd)	$PM_{2.5}$ ($\mu g/m^3$)	SO_4^{2-} ($\mu g/m^3$)	NO_3^- ($\mu g/m^3$)	NH_4^+ ($\mu g/m^3$)	OA ($\mu g/m^3$)	EC ($\mu g/m^3$)	ALWC ($\mu g/m^3$)	O:C	ambient RH (%)	phase state	
											25th–75th	mean
						Seoul						
2020	12/21	31.1	2.5	9.5	4.0	5.9	1.0	13.2	0.40	65.7	liquid–semisolid	semisolid
	12/22	37.1	3.2	13.8	5.9	6.8	1.1	18.2	0.42	66.7	lquid–semisolid	liquid
	12/23	60.8	5.2	22.5	9.7	10.4	1.8	50.5	0.41	77.2	liquid	liquid
	12/24	17.0	2.2	3.4	1.7	5.7	0.7	3.8	0.40	54.8	semisolid	semisolid
	12/26	43.3	3.3	15.0	6.3	9.5	1.3	16.2	0.41	65.0	liquid–semisolid	semisolid
	12/27	33.3	3.2	11.1	5.1	8.4	1.0	16.7	0.41	66.0	liquid–semisolid	liquid
	12/28	46.1	3.6	16.7	7.0	11.2	1.5	25.6	0.41	70.4	liquid	liquid
	12/29	34.0	3.9	7.0	3.8	10.7	1.4	12.9	0.42	63.9	semisolid	semisolid
2021	01/01	15.0	1.3	3.4	1.5	3.6	0.6	3.6	0.40	53.5	semisolid	semisolid
	01/02	12.7	1.1	1.2	0.6	2.9	0.5	0.9	0.39	42.8	semisolid	semisolid
	01/11	34.0	2.5	8.1	3.6	10.4	1.3	9.3	0.39	63.2	liquid–semisolid	semisolid
	01/12	41.9	4.9	11.4	5.6	9.7	1.1	74.1	0.40	85.9	liquid	liquid
	01/13	38.0	2.9	7.7	3.0	10.1	1.3	14.1	0.41	70.4	semisolid	semisolid
average		34.2	3.1	10.1	4.4	8.1	1.1	19.9	0.41	65.0		
						Beijing						
2020	12/21	48.3	3.7	12.5	6.5	11.9		3.9	0.42	33.8	semisolid	semisolid
	12/22	58.8	4.0	13.5	7.2	14.0		4.2	0.40	32.9	semisolid	semisolid
	12/28	44.9	4.3	10.3	5.3	10.5		7.0	0.40	30.5	semisolid	semisolid
	12/29	18.5	0.7	0.3	0.4	1.7		0.1	0.36	15.7	(semi)solid	(semi) solid
2021	01/01	40.7	3.1	8.2	4.8	12.4		3.8	0.40	33.4	semisolid	semisolid
	01/02	45.8	4.5	9.5	5.8	9.1		4.8	0.40	29.5	semisolid	semisolid
	01/11	24.5	1.3	1.9	1.4	4.1		0.5	0.39	24.4	semisolid	semisolid
	01/12	48.6	1.7	6.7	3.5	8.8		0.9	0.38	23.5	semisolid	semisolid
	01/13	55.7	4.3	7.2	4.4	7.0		8.8	0.40	38.2	semisolid	semisolid
average		42.9	3.1	7.8	4.4	8.8		3.8	0.39	29.1		

[a]Chemical compositions of the inorganic and carbonaceous species were measured for $PM_{2.5}$ in Seoul and for $PM_{1.0}$ in Beijing. Phase states of liquid, semisolid, or (semi)solid of $PM_{2.5}$ filter samples at 290–293 K at ambient RH between the 25th and 75th percentile level and on mean value are also included.

Some studies on phase states of real-world aerosol particles have been conducted under different environments.[20−26] In a rural area in the southeastern United States,[20] PM was reported to mostly exist in a liquid state. In Shenzhen, a coastal city in China, submicrometer-sized particles were observed to be in the liquid state under high RH > ∼60% and high inorganic mass fraction.[24] In Beijing, when heavy haze episodes occurred during winter, a phase transition of submicrometer particles from a semisolid to a liquid state was observed.[25] This phenomenon was explained by the concurrent enhanced RH and inorganic fraction in aerosol particles that promoted higher ALWC and thereby lowering the viscosity. On the contrary, in central Amazonia, nonliquid PM was predominant even under high RH conditions during a period of urban pollution and biomass burning.[26] These studies notwithstanding, information on the phase state of atmospheric particles remains largely unknown. More data are needed to understand the typical range of physical properties exhibited by PM and also to examine how the physical properties are linked to PM pollution.

Herein, we collected $PM_{2.5}$ filter samples simultaneously from two megacities, Seoul and Beijing, during the 2020–2021 winter. In the laboratory, the morphology and phase behavior of $PM_{2.5}$ upon dehydration were observed using the filter extracts from the two cities by optical microscopy combined with a poke-and-flow technique at temperatures of 290–293 K. Based on the observations, we classified the phase states of the bulk of $PM_{2.5}$ in the urban environments of Seoul and Beijing. Moreover, the relationship between the phase states and chemical composition of $PM_{2.5}$ was investigated with consideration of the ALWC and RH. Finally, the results of the analysis of the $PM_{2.5}$ phase state were applied to determine its interplay with the observed particle size distributions in these megacities.

2. METHODOLOGY

2.1. Measurement Sites and Collection of $PM_{2.5}$ Samples. $PM_{2.5}$ quartz-filter samples (8 × 10 in., Pall Corporation, product no. 7204) were collected daily from 10:00 to 09:00 a.m. of the following day in local time, using high-volume air samplers at a flow rate of ∼1000 L min^{-1} (SIBATA, HV-1000R, Japan) simultaneously at a metropolitan area intensive air quality monitoring site in Bulgwang-dong, Eunpyeong-gu in Seoul (37.61°N, 126.93°E) and at the Changping campus of Peking University in Beijing (40.25°N, 116.19°E) from Dec 15, 2020 to Jan 14, 2021 (Figure S1). Details of the sites are described in Section S1. After collection, the filters were stored at ∼255 K and used for analysis within ∼1 month.

During the entire period, we selected samples from both sites for phase state determinations of the $PM_{2.5}$, which included the beginning of the increase in $PM_{2.5}$ concentration

https://doi.org/10.1021/acs.est.2c06377
Environ. Sci. Technol. 2022, 56, 17581−17590

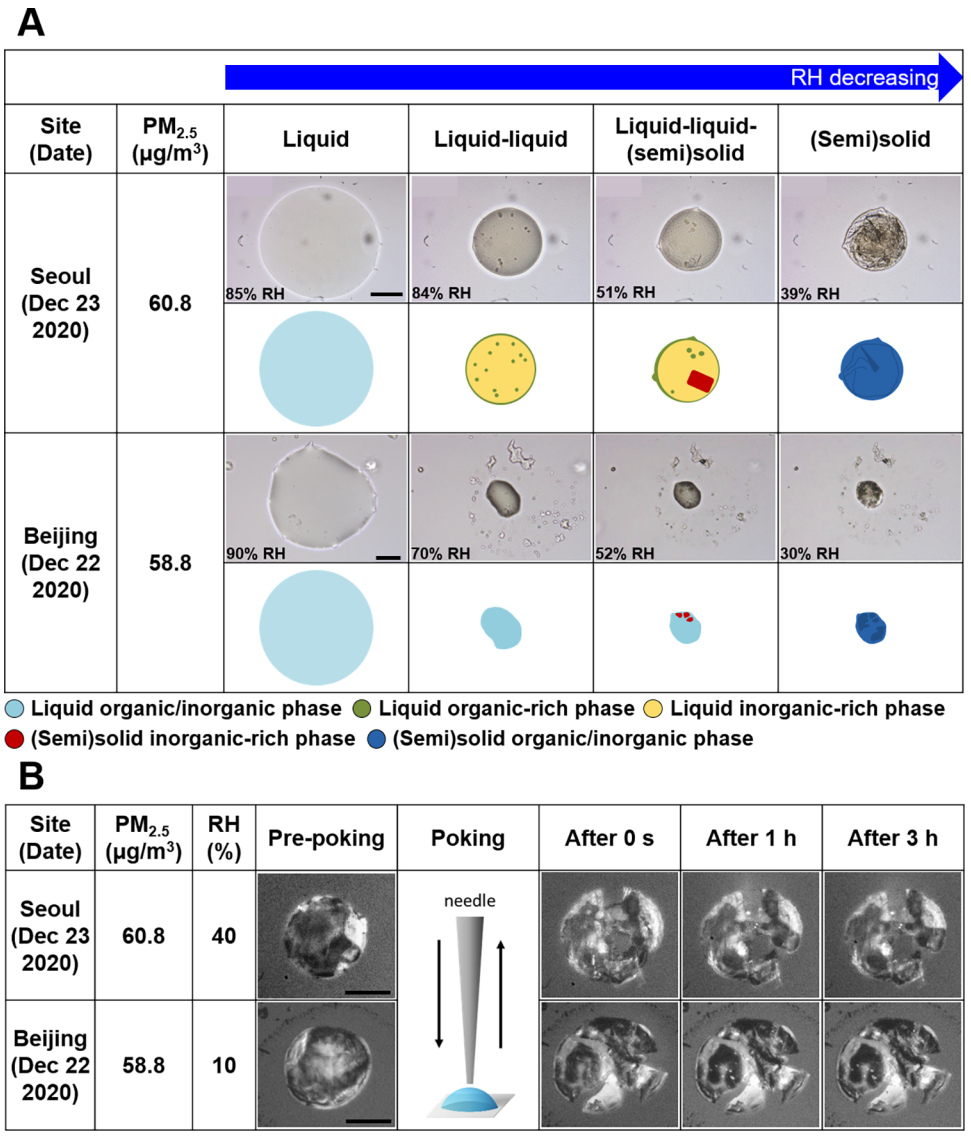

Figure 1. Morphology and phase behavior of $PM_{2.5}$ in Seoul and Beijing. (A) Optical images upon dehydration of $PM_{2.5}$ samples were the highest daily average concentration in Seoul and Beijing at 290 K. Illustrations are given for interpretation of the optical images. Light blue: single liquid mixed organic/inorganic phase; green and yellow: liquid organic-rich and liquid inorganic-rich phases, respectively; red: (semi)solid inorganic-rich phase; and dark blue: (semi)solid organic/inorganic phase. (B) Optical images at 293 K on pre-poking, poking, and post-poking of the same $PM_{2.5}$ filter samples as shown in (A). The solid black scale bars in (A) and (B) indicate 20 μm.

and several $PM_{2.5}$ pollution episodes with daily mean $PM_{2.5}$ concentrations > 35 $\mu g/m^3$, based on the Korean daily air quality standard for $PM_{2.5}$.[27] Figure S2 shows the four cases (Cases 1−4) of the most polluted episodes. In total, 22 samples (13 samples from Seoul and 9 from Beijing) were analyzed for phase states (Section S2). Samples collected from Beijing on Dec 23, 24, 26, and 27, 2020 were excluded owing to very low surface tension of the droplets on a hydrophobic substrate, making them unsuitable for optical microscopy experiments. The information on samples, their chemical composition, and meteorological parameters (Section S3) for Cases 1−4 is summarized in Table 1. Note that $PM_{2.5}$ mass concentrations were measured in both cities, but chemical compositions were measured for the $PM_{2.5}$ size range in Seoul and for the $PM_{1.0}$ size range in Beijing (Section S3). The majority of the particles were in the accumulation mode (i.e., ~200−500 nm) in the two cities, and thus, the $PM_{2.5}$ and $PM_{1.0}$ account likely for the majority of the particle mass within the fine mode in each city.[28]

2.2. Morphology Observation Using Optical Microscopy. The morphology of $PM_{2.5}$ for Cases 1−4 from Seoul and Beijing was assessed using optical microscopy at 290 ± 1 K. Note that the temperature used for the laboratory evaluation allows for a consistent comparison of material properties in both cities; however, it differs from the actual temperature which would be typical (and distinct) for each city during winter. A detailed description of the method and procedure of the optical microscopy has been reported in previous work.[29−31] Briefly, $PM_{2.5}$ droplets deposited on the substrate were equilibrated in a flow cell at ~100% RH for 20 min after which the RH was reduced to ~0% at a rate of ~0.5% RH min^{-1} by adjusting the ratio of N_2 and H_2O gas flows (total flow: 500 sccm). The changes in the morphology of the droplets were observed using an optical microscope (Olympus BX43, 40 objective, Japan) and monitored/recorded every 10 s

https://doi.org/10.1021/acs.est.2c06377
Environ. Sci. Technol. 2022, 56, 17581−17590

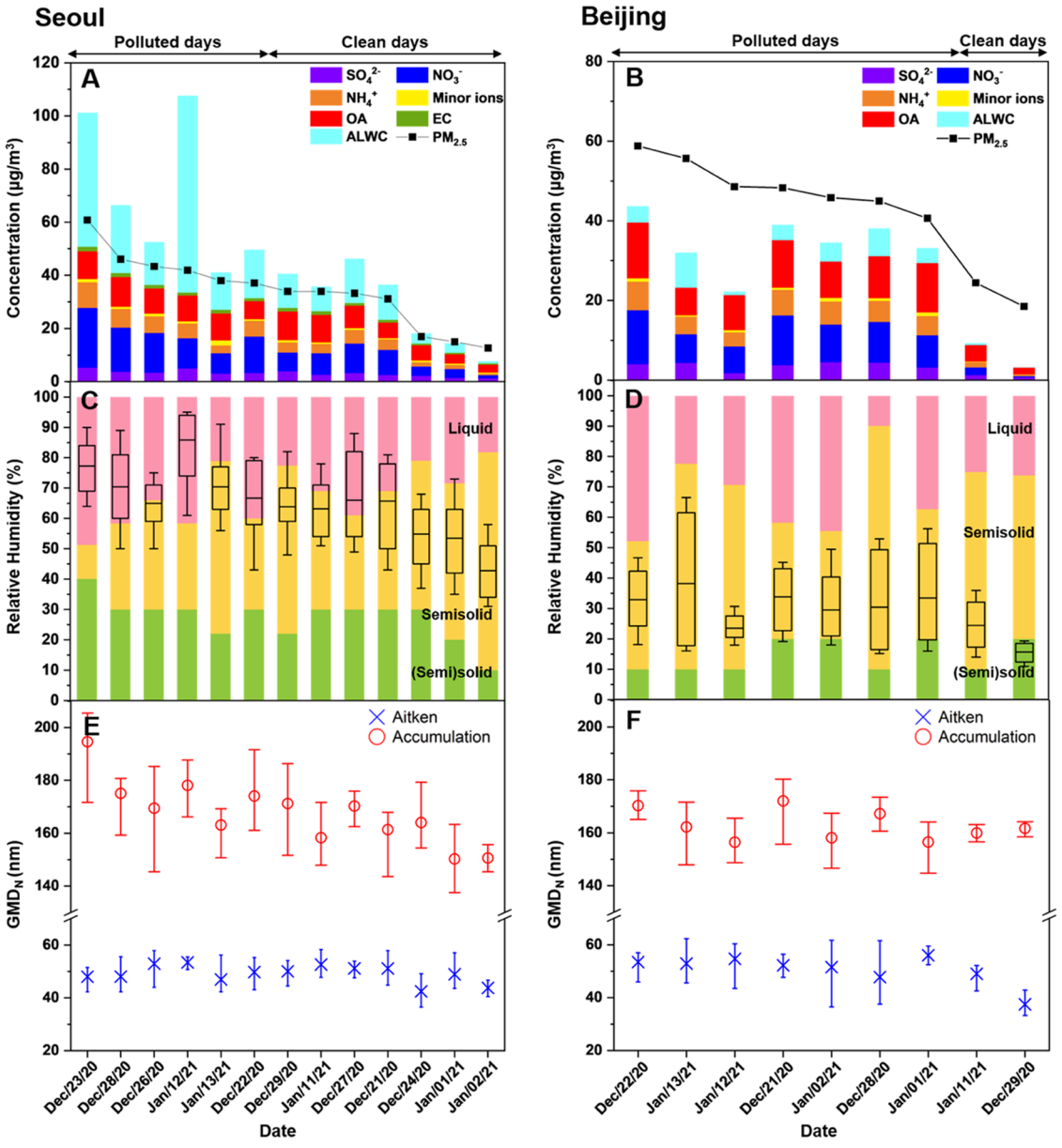

Figure 2. Daily average chemical composition and aerosol liquid water content (ALWC) of (A) $PM_{2.5}$ in Seoul and (B) $PM_{1.0}$ in Beijing. The minor ions of $PM_{2.5}$ in Seoul indicate the sum of Cl^-, Na^+, K^+, Mg^{2+}, and Ca^{2+} and of $PM_{1.0}$ in Beijing indicate Cl^-. The daily phase state of $PM_{2.5}$ filter samples as a function of relative humidity (RH) are shown in (C) and (D). The pink, yellow, and green areas represent liquid, semisolid, and (semi)solid phase states, respectively. The black box plots in (C) and (D) represent the ambient RH in Seoul and Beijing. The boxes indicate the mean, 25th, and 75th percentiles, and the whiskers show the minimum and maximum values. (E) and (F) show the geometric number mean diameters (GMD_N) of Aitken (20−100 nm) and accumulation (100−470 nm) mode of each hourly averaged particle size distribution for Seoul and Beijing, respectively. Dates are arranged in order from high to low daily mean $PM_{2.5}$ concentrations (black line in (A) and (B)).

during the experiment using a charge-coupled device (CCD) camera (DigiRetina 16, Tucsen, China).

2.3. Determination of (Semi)Solid Phases of $PM_{2.5}$ Using the Poke-and-Flow Technique. Poke-and-flow experiments were conducted to determine the approximate viscosity of semisolid or solid phases, henceforth referred to as "(semi)solid", of $PM_{2.5}$ droplets for Cases 1−4 at 293 ± 1 K.[32,33] The experimental procedure of the poke-and-flow technique has been described in detail previously.[13,33−35] In brief, a hydrophobic substrate with deposited droplets was kept in a RH-controlled flow cell. The droplets were equilibrated at ∼100% RH, and then, the RH was reduced to ∼40% at ∼1% RH min^{-1}. Next, the droplets were poked by a fine needle (Jung Rim Medical Industrial, South Korea) at ∼40, ∼30, ∼20, ∼10%, or ∼0% RH to find the RH at which the droplets started to crack. Prior to poking, the droplets were equilibrated for ∼1 h at the target RH. Once particles cracked upon a poking action, they were monitored for ∼3 h to check the occurrence of any changes due to fluid flow using a CCD camera (Hamamatsu, C11440-42U30, Japan). If no fluid flow was detected, the lower limit of viscosity of the sample was defined as ∼10^8 Pa s,[8,33,34,36] corresponding to a (semi)solid state.[5] In this study, using the poke-and-flow technique, we could not determine the viscosity range of semisolid particles (10^2 to 10^8 Pa s) to a more precise degree because the real-world aerosols were supersaturated with respect to inorganic

https://doi.org/10.1021/acs.est.2c06377
Environ. Sci. Technol. 2022, 56, 17581−17590

salts (e.g., ammonium sulfate) at the intermediate and low RH levels probed.

3. RESULTS AND DISCUSSION

3.1. Observation of Morphology and Phase Behavior of $PM_{2.5}$ in Seoul and Beijing. The phase behavior and the resulting phase state of $PM_{2.5}$, collected simultaneously in Seoul and Beijing during the winter of 2021−2022, including high $PM_{2.5}$ events in the two megacities (Cases 1−4), were investigated. Microscopy analysis revealed different and complex morphologies of the $PM_{2.5}$ filter samples with decreasing RH. Figure 1A shows a set of representative optical images of morphological changes in $PM_{2.5}$ upon dehydration for the sample collected in Seoul on Dec 23, 2020, when the $PM_{2.5}$ mass concentration was the highest. The probed $PM_{2.5}$ "bulk" droplet existed as a single liquid phase at >∼85% RH, and at ∼84% RH, the droplets underwent liquid−liquid phase separation (LLPS), leading to a core-shell morphology (Figure 1A). Such a phase separation can be explained by the range of the average oxygen-to-carbon ratios (O:C) of organic materials (∼0.4, Table 1 and Section S4); in laboratory studies, LLPS commonly occurs for O:C < 0.8 when dissolved aqueous inorganics like ammonium and sulfate ions are present.[6,37,38] Interestingly, a sudden appearance of a crystal was observed at a lower RH of ∼51% in the interior of the $PM_{2.5}$ droplet (Figure 1A), resulting in the coexistence of two liquid phases and one solid phase, here denoted as liquid−liquid−(semi)-solid state. Recently, Gaikwad et al.[32] also observed such a liquid−liquid−(semi)solid state of $PM_{2.5}$ collected from a rural site during winter. They inferred the (semi)solid state to be composed of inorganic salts, such as ammonium sulfate, ammonium nitrate, or sodium chloride, based on the shape and the RH level of its initial occurrence during dehydration. Huang et al.[12] observed three coexisting phases in the liquid−liquid−liquid-phase-separated aerosol particles in their laboratory study involving mixtures of materials serving as proxies for primary organic aerosol, SOAs, and SIAs. To the best of our knowledge, this coexistence of three phases in real-world aerosol particles has not been reported for polluted or clean environments. Such morphological analysis of atmospheric aerosols could provide further insights into the atmospheric chemistry and formation/growth of particles, and additional studies are needed in this regard. The liquid−liquid−(semi)solid multiphase state of the Seoul $PM_{2.5}$ existed until the inorganic fraction of the particle effloresced at ∼39% RH (Figure 1A).

The morphology and phase behavior of $PM_{2.5}$ in Beijing were much more complicated than those of $PM_{2.5}$ in Seoul. Optical images of the Beijing $PM_{2.5}$ sampled during the highest aerosol mass concentration episode, recorded upon dehydration, are shown in Figure 1A. The single $PM_{2.5}$ droplet at high RH got smaller upon dehydration; however, an irregular morphology was maintained during the dehydration process, unlike a sphere or rounded shape observed in the samples from Seoul (although the daily mean $PM_{2.5}$ concentration was similar in the two cities). Moreover, LLPS in the Beijing $PM_{2.5}$ was not detectable in the microscopy observations even though the O:C ratio was ∼0.4 (Table 1). This was likely due to the irregular morphology and low surface tension of the droplet,[39,40] which was abundant in organic materials (Figures 2A,B and S3). At lower RH, crystals appeared abruptly in the particle, and then the inorganic fraction of the particle effloresced at ∼30% RH (Figure 1A). Similar phase behavior and morphology of $PM_{2.5}$ droplets were also observed for other $PM_{2.5}$ samples from Seoul and Beijing (Figure S4).

To examine the presence and/or onset of a (semi)solid phase state, the poke-and-flow technique was used.[13,33,34] All $PM_{2.5}$ particles, including the same $PM_{2.5}$ sample as shown in Figure 1A and S4, did crack upon poking with a needle, and no return flow and associated shape change were observable thereafter for ∼3 h in the optical images (Figures 1B and S5). This process indicates a (semi)solid phase state with viscosity values > $\sim 10^8$ Pa s.[8,33,34,36] It should be noted that the RH at which the particles cracked was different in samples from Seoul and Beijing, as shown in Figures 1B and S5, being higher for samples from Seoul (RH range: ∼20−30%) than for those from Beijing (RH range: ∼10−20%). This is probably due to the greater mass fraction of inorganic substances in the Seoul samples. The effect of inorganic salts on the phase state in internally mixed organic/inorganic aerosol particles has been reported previously.[10,13]

Based on the results of the optical microscopy and poke-and-flow experiments, in this study, we categorized the phase states of the bulk of $PM_{2.5}$ material in Seoul and Beijing as follows: (1) "liquid" in the cases of single liquid or liquid−liquid-phase-separated particles, (2) "semisolid" in the case of liquid−liquid−(semi)solid multiphase particles (although not all phases were necessarily semisolid), and (3) "(semi)solid" in the case of semisolid or more likely solid particles.

Summarized in Figure 2A−D are the chemical compositions ($PM_{2.5}$ for Seoul and $PM_{1.0}$ for Beijing) and phase states of the $PM_{2.5}$ over the whole RH range defined by the three categories in the two cities. In this figure, dates are arranged in order from high to a low daily average of mass concentration of $PM_{2.5}$. In Seoul, the $PM_{2.5}$ was in the liquid state for RH > ∼68%, in the semisolid state for ∼27% < RH < ∼68%, and in the (semi)solid state for RH < ∼27% on average during Cases 1−4, with some variations on each date (Figure 2C). In Beijing, the $PM_{2.5}$ was in the liquid-phase state for RH > ∼68%, in the semisolid state for ∼14% < RH < ∼68%, and in the (semi)solid state for RH < ∼14% during Cases 1−4 (Figure 2D). The RH range for the liquid-phase state was similar in the two cities, but that for a physical state categorized as being at the boundary of (semi)solid was higher in Seoul than in Beijing.

3.2. Comparison of the Phase States of $PM_{2.5}$ in Seoul and Beijing. To characterize the phase state of the $PM_{2.5}$ in the urban atmosphere in Seoul and Beijing during the measurement period, we first compared the determined phase states to the ambient RH recorded in the cities. Figure 2C,D shows box plots of daily ambient RH ranges for the two cities. The boxes indicate the daily mean, 25th, and 75th percentiles, and the whiskers represent the minimum and maximum. The daily mean ambient RH was remarkably different in the two cities, being ∼65.0 ± 10.3% in Seoul and ∼29.1 ± 6.4% in Beijing during Cases 1−4. The phase state of the bulk of $PM_{2.5}$ from the two megacities was determined based on the ambient RH (mean value of the box plot in Figure 2C,D, and Table 1) and from the measured phase states of $PM_{2.5}$ as a function of RH at 290−293 K (see Section 3.1). During that winter, $PM_{2.5}$ existed in a liquid or semisolid phase state in Seoul but was semisolid or (semi)solid in Beijing. The results indicate significantly different phase states in the two urban environments. This observation clearly suggests that the $PM_{2.5}$ in Seoul has a lower viscosity than that of the $PM_{2.5}$ in Beijing when evaluated at the same temperature. We also

https://doi.org/10.1021/acs.est.2c06377
Environ. Sci. Technol. 2022, 56, 17581−17590

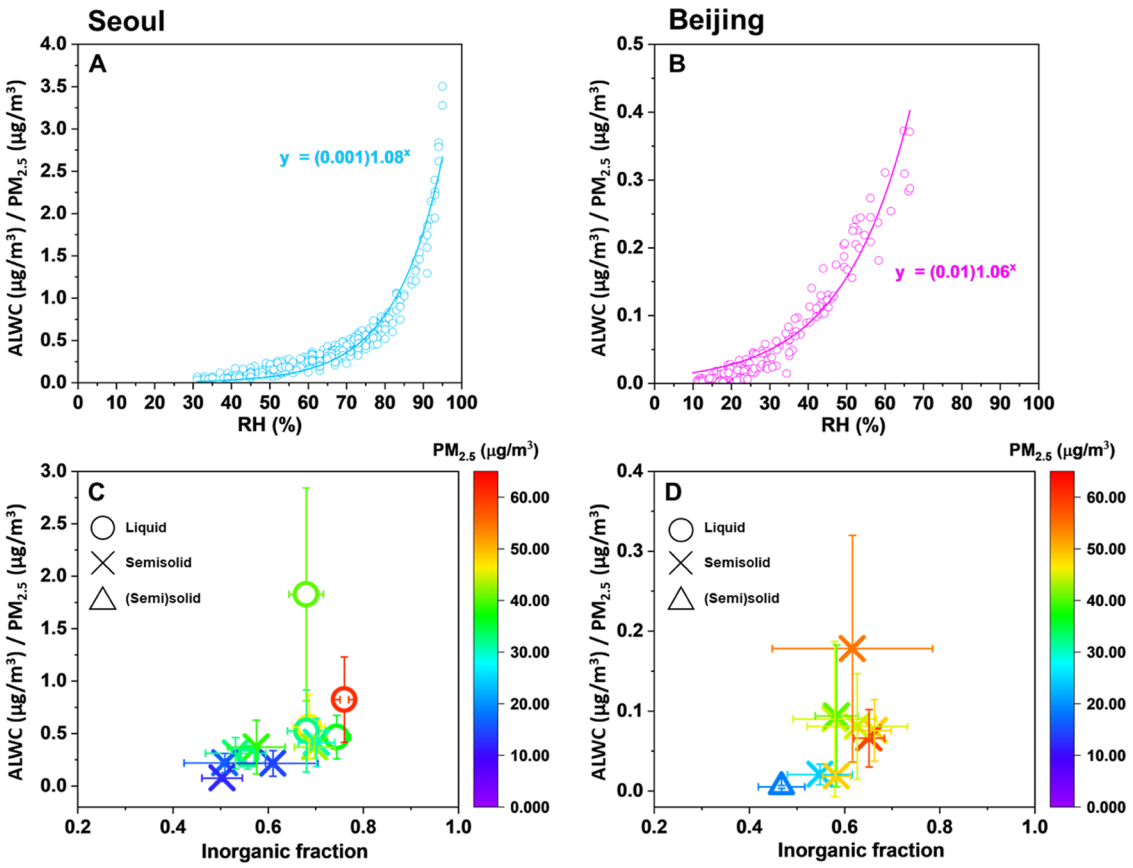

Figure 3. Hourly aerosol liquid water content (ALWC)/$PM_{2.5}$ as a function of ambient relative humidity (RH) in (A) Seoul and (B) Beijing during Cases 1−4. Daily ALWC/$PM_{2.5}$ as a function of the inorganic mass fraction of (C) $PM_{2.5}$ in Seoul and (D) $PM_{1.0}$ in Beijing. Phase states of the bulk of $PM_{2.5}$ determined at 290−293 K are also included. The error bars of *x*- and *y*-axis in (C) and (D) are from the standard deviation of hourly data of inorganic mass fraction and ALWC/$PM_{2.5}$.

compared this finding using a different technique that of impactor-based rebound experiments in the field at ambient conditions, as described in the Supporting Information (Section S5). As shown in Figure S6A,B, the phase states on each date in Beijing determined using the two different techniques were in good agreement although the particle size ranges were different ($PM_{2.5}$ vs ∼300 nm).

Liu et al.[25] showed that ambient particles monitored in Beijing had a (semi)solid-like behavior during winter based on the rebound fraction measurement, which is similar to the observations in the present study. Based on the results of a laboratory study, Song et al.[41] inferred a long mixing time (>100 h) within toluene-derived SOA in Beijing using the viscosity and employing the Stokes−Einstein equation. Notably, the phase state of $PM_{2.5}$ was significantly different on polluted and clean days in Seoul: the liquid state was dominant on polluted days, whereas the semisolid phase state was dominant on clean days (Figure 2C). On polluted days in Seoul, high RH, with average values > ∼73%, was observed (Table 1). Such conditions, with RH greater than deliquescence of ammonium nitrate[42] (which was the major compound in $PM_{2.5}$ on polluted days in this study, Figure S3A), could accelerate chemical reaction with surrounding gas molecules leading to enhanced $PM_{2.5}$ mass concentration.

The phase states of particles are primarily sensitive not only to RH but also to the chemical composition.[24,43,44] Using the chemical composition and meteorological parameters, we calculated the ALWC for the two cities (Section S6). Figure 3A,B shows the ALWC/$PM_{2.5}$ and ambient RH in Seoul and Beijing, respectively. The ALWC/$PM_{2.5}$ increased with the RH in both the cities (the ALWC was much higher at the Seoul site (19.9 ± 19.7 $\mu g/m^3$), compared with that at the Beijing site (3.8 ± 2.8 $\mu g/m^3$), Table 1). The relationship between the inorganic fraction, ALWC, and phase state of $PM_{2.5}$ is displayed in Figure 3C,D. When the inorganic fraction was greater than ∼0.7, the ALWC/$PM_{2.5}$ was significantly increased and the particles were in the liquid state. In Seoul, $PM_{2.5}$ tended to be liquid-like because the inorganic fraction and ALWC/$PM_{2.5}$ were enhanced. This indicates that the abundant ALWC lowered the viscosity of the $PM_{2.5}$, forming a liquid phase during winter. Liu et al.[24] also observed this phase behavior at a coastal region; they showed that atmospheric aerosol was predominantly in the liquid phase under high ambient RH and ALWC, with an abundance of inorganic ions. A recent study by Gkatzelis et al.[45] focused on the phase state and SOA pollution in Beijing during winter and reported a relationship between SOA, phase states, and ALWC. They showed that 15−25% of the SOA mass was enhanced by the gas-to-particle partitioning on liquid particles during the organic particulate pollution. More studies are needed to explore how a phase state of organic aerosols derives $PM_{2.5}$ pollution.

In addition to RH and the aerosol composition, the phase state can also strongly depend on temperature.[14,44,46,47] Kasparoglu et al.[14] showed that the viscosity of sucrose solution increased by 2−3 orders of magnitude for a 20 K

https://doi.org/10.1021/acs.est.2c06377
Environ. Sci. Technol. 2022, 56, 17581−17590

decrease in temperature. In this study, the average ambient temperature was ~270 ± 6 K in Seoul and ~269 ± 4 K in Beijing during the study period, which is relatively lower than the experimental temperature. This indicates that the viscosity of $PM_{2.5}$ maybe is higher in Seoul and Beijing. However, the effect of temperature on the viscosity and phase state of real-world PM has not been studied. For this reason, we have limited the current analysis to the experimental temperature of ~290 K. Further studies are warranted to determine the effect of temperature on the phase state of $PM_{2.5}$.

3.3. Effect of Phase States on the Size Distribution of Particles. Several recent laboratory and modeling studies have shown that the phase state of particles can affect the particle size distribution.[18,19,48,49] Liquid particles can enable the accommodation and partitioning of gas molecules into the entire particle volume with a rapid uptake/reaction of atmospheric gas molecules. Specifically, liquid particles can grow easily in the accumulation mode with the instantaneous equilibrium regardless of their size. In contrast, in the case of solid particles, the process is different that gas molecules can only be partitioned onto their surface. (Semi)solid particles can resist growth in the accumulation mode due to severe diffusion limitation, whereas in the Aitken mode, they may grow relatively quickly because the diffusion time scale depends on the square of the particle diameter.[49]

We investigated whether the phase states of $PM_{2.5}$ influenced particle size distribution in Seoul and Beijing (Section S7). Figure S7 illustrates the particle number and volume size distributions of $PM_{2.5}$ (20−470 nm) with 5 min time resolution in Seoul and Beijing during the entire measurement period. To compare the characteristics of $PM_{2.5}$ growth in the Aitken (20−100 nm) and accumulation (100−470 nm) modes based on the phase states of $PM_{2.5}$ in the two cities, the geometric number mean diameter (GMD_N) of the two modes was calculated from the particle number size distribution (details are given in Section S7).

Shown in Figure 2E,F are the plots for the daily average GMD_N of the Aitken (20−100 nm) and accumulation (100−470 nm) modes in Seoul and Beijing, respectively. In Seoul, in the liquid phase of the bulk of $PM_{2.5}$, the mean GMD_N of the accumulation mode was clearly higher compared to that of the semisolid phase state (Figure 2E). This infers that liquid aerosol particles grew easily with fast equilibrium between surrounded gas molecules and the liquid droplet, resulting in the enhanced GMD_N of the accumulation mode. The higher average GMD_N on $PM_{2.5}$ polluted days in Seoul was presumed to be due to particle growth caused by various processes of active chemical reactions, condensation, or coagulation in the liquid phase. In contrast, in Beijing, no obvious variation of the average GMD_N in the accumulation mode was observed in the semisolid $PM_{2.5}$, which was predominant on most days (Figure 2F). This is likely due to insufficient growth conditions that slowed chemical reactions occurring on the surface and/or less gas-phase oxidation of organic and subsequent portioning to semisolid particles.[50,51] This is consistent with previous calculations that have shown a similar decrease in geometric mean particle size (or volume) of accumulation mode for cases of more viscous particles.[18,19,48,49,52] In the Aitken mode, a remarkable variation of the mean GMD_N on the different phase states was not observed in either city (Figure 2E,F). This is attributed to the averaged measurement data of $PM_{2.5}$, which were largely influenced by the accumulation mode particles. Thus, the phase states of the $PM_{2.5}$ would be effective for the accumulation mode particles and not for the nucleation mode particles. A similar pattern was observed for the geometric volume diameter (GMD_V) of the two modes for both cities (Figure S8).

Herein, we reveal the range of phase states of $PM_{2.5}$ in two megacities of northeast Asia and their impact on the particle size distribution in the accumulation mode based on field measurements during winter. Prevailing ambient temperature and RH could also impact the size distribution, which in turn would impact the phase state. Thus, further studies are needed to confirm this pattern under different environmental conditions, including different seasons.

■ ASSOCIATED CONTENT

Supporting Information

The Supporting Information is available free of charge at https://pubs.acs.org/doi/10.1021/acs.est.2c06377.

Site description (Section S1); preparation of drops of $PM_{2.5}$ (Section S2); chemical compositions and meteorological parameters (Section S3); analysis of oxygen-to-carbon ratios (Section S4); rebound fraction (Section S5); calculation of aerosol liquid water content (Section S6); particle number size distribution (Section S7); location of sampling sites (Figure S1); the $PM_{2.5}$ concentration during winter period in Seoul and Beijing (Figure S2); mass concentration and major chemical species of $PM_{2.5}$ and $PM_{1.0}$ for the Seoul and Beijing (Figure S3); optical images of $PM_{2.5}$ concentrations in Seoul and Beijing (Figure S4); pre-poking, poking, and post-poking optical images of $PM_{2.5}$ in Seoul and Beijing (Figure S5); a comparison of the daily phase state of ambient particles in Beijing from microscopic observation combined with a poke-and-flow technique and rebound fraction (Figure S6); particle number and volume size distributions (Figure S7); particle geometric volume mean diameters (Figure S8) (PDF)

■ AUTHOR INFORMATION

Corresponding Author

Mijung Song − *Department of Environment and Energy, Jeonbuk National University, Jeonju-si 54896 Jeollabuk-do, Republic of Korea; Department of Earth and Environmental Sciences, Jeonbuk National University, Jeonju-si 54896 Jeollabuk-do, Republic of Korea;* orcid.org/0000-0001-9612-1998; Email: Mijung.Song@jbnu.ac.kr

Authors

Rani Jeong − *Department of Environment and Energy, Jeonbuk National University, Jeonju-si 54896 Jeollabuk-do, Republic of Korea*

Daeun Kim − *Department of Environment and Energy, Jeonbuk National University, Jeonju-si 54896 Jeollabuk-do, Republic of Korea*

Yanting Qiu − *State Key Joint Laboratory of Environmental Simulation and Pollution Control, College of Environmental Sciences and Engineering, Peking University, Beijing 100871, China*

Xiangxinyue Meng − *State Key Joint Laboratory of Environmental Simulation and Pollution Control, College of Environmental Sciences and Engineering, Peking University, Beijing 100871, China*

https://doi.org/10.1021/acs.est.2c06377
Environ. Sci. Technol. 2022, 56, 17581−17590

Zhijun Wu − *State Key Joint Laboratory of Environmental Simulation and Pollution Control, College of Environmental Sciences and Engineering, Peking University, Beijing 100871, China;* orcid.org/0000-0001-8910-5674
Andreas Zuend − *Department of Atmospheric and Oceanic Sciences, McGill University, Montréal, Québec H3A 0B9, Canada;* orcid.org/0000-0003-3101-8521
Yoonkyeong Ha − *School of Civil and Environmental Engineering, Pusan National University, Busan 46241, Republic of Korea*
Changhyuk Kim − *School of Civil and Environmental Engineering, Pusan National University, Busan 46241, Republic of Korea*
Haeri Kim − *Department of Environment and Energy, Jeonbuk National University, Jeonju-si 54896 Jeollabuk-do, Republic of Korea*
Sanjit Gaikwad − *Department of Environment and Energy, Jeonbuk National University, Jeonju-si 54896 Jeollabuk-do, Republic of Korea*
Kyoung-Soon Jang − *Bio-Chemical Analysis Team, Korea Basic Science Institute, Cheongju 28119, Republic of Korea*
Ji Yi Lee − *Department of Environmental Science & Engineering, Ewha Womans University, Seoul 03760, Republic of Korea*
Joonyoung Ahn − *Department of Atmospheric Environment Research, National Institute of Environmental Research, Seoul 03367, Republic of Korea*

Complete contact information is available at: https://pubs.acs.org/10.1021/acs.est.2c06377

Author Contributions

M.S. designed this study. M.S., R.J., D.K., Y.Q., Z.W., Y.H., C.K., H.K., K.-S.J., J.Y.L., and J.A. conducted measurements and analyzed the data. M.S., R.J., A.Z., C.K., D.K., H.K., and S.G. prepared the manuscript with the contributions of all co-authors. All authors have read and agreed to the published version of the manuscript.

Funding

This work was supported by the Fine Particle Research Initiative in East Asia Considering National Differences (FRIEND) Project (NRF-2020M3G1A1114548) and by the National Research Foundation of Korea (NRF) grant funded by the Korean government (MSIT) (NRF-2019R1A2C1086187).

Notes

The authors declare no competing financial interest.

■ ACKNOWLEDGMENTS

M.S. thanks to Hyeokjin Kim and Dohyun Kim for the technical support.

■ REFERENCES

(1) Wu, J.; Bei, N.; Hu, B.; Liu, S.; Wang, Y.; Shen, Z.; Li, X.; Liu, L.; Wang, R.; Liu, Z.; Cao, J.; Tie, X.; Molina, L. T.; Li, G. Aerosol-photolysis interaction reduces particulate matter during wintertime haze events. *Proc. Natl. Acad. Sci. U.S.A.* **2020**, *117*, 9755−9761.
(2) Bhattarai, G.; Lee, J. B.; Kim, M.-H.; Ham, S.; So, H.-S.; Oh, S.; Sim, H.-J.; Lee, J.-C.; Song, M.; Kook, S.-H. Maternal exposure to fine particulate matter during pregnancy induces progressive senescence of hematopoietic stem cells under preferential impairment of the bone marrow microenvironment and aids development of myeloproliferative disease. *Leukemia* **2020**, *34*, 1481−1484.
(3) Masson-Delmotte, V.; P Zhai, A. P.; Connors, S. L.; Péan, C.; Berger, S.; Caud, N.; Chen, Y.; Goldfarb, L.; Gomis, M. I.; Huang, M.; Leitzell, K.; Lonnoy, E.; Matthews, J. B. R.; Maycock, T. K.; Waterfield, T.; Yelekçi, O.; Yu, R.; a. B. Z. e. C. U. P. I. P. IPCC. *Climate Change: The Physical Science Basis 2021, Contribution of Working Group I to the Sixth Assessment Report of the Intergovernmental Panel on Climate Change*, 2021.
(4) Martin, S. T. Phase transitions of aqueous atmospheric particles. *Chem. Rev.* **2000**, *100*, 3403−3454.
(5) Koop, T.; Bookhold, J.; Shiraiwa, M.; Pöschl, U. Glass transition and phase state of organic compounds: dependency on molecular properties and implications for secondary organic aerosols in the atmosphere. *Phys. Chem. Chem. Phys.* **2011**, *13*, 19238−19255.
(6) Krieger, U. K.; Marcolli, C.; Reid, J. P. Exploring the complexity of aerosol particle properties and processes using single particle techniques. *Chem. Soc. Rev.* **2012**, *41*, 6631−6662.
(7) Power, R. M.; Simpson, S.; Reid, J.; Hudson, A. The transition from liquid to solid-like behaviour in ultrahigh viscosity aerosol particles. *Chem. Sci.* **2013**, *4*, 2597−2604.
(8) Song, M.; Maclean, A. M.; Huang, Y.; Smith, N. R.; Blair, S. L.; Laskin, J.; Laskin, A.; DeRieux, W.-S. W.; Li, Y.; Shiraiwa, M.; Nizkorodov, S. A.; Bertram, A. K. Liquid−liquid phase separation and viscosity within secondary organic aerosol generated from diesel fuel vapors. *Atmos. Chem. Phys.* **2019**, *19*, 12515−12529.
(9) Rovelli, G.; Song, Y.-C.; Maclean, A. M.; Topping, D. O.; Bertram, A. K.; Reid, J. P. Comparison of approaches for measuring and predicting the viscosity of ternary component aerosol particles. *Anal. Chem.* **2019**, *91*, 5074−5082.
(10) Richards, D. S.; Trobaugh, K. L.; Hajek-Herrera, J.; Price, C. L.; Sheldon, C. S.; Davies, J. F.; Davis, R. D. Ion-molecule interactions enable unexpected phase transitions in organic-inorganic aerosol. *Sci. Adv.* **2020**, *6*, No. eabb5643.
(11) Song, Y.-C.; Lilek, J.; Lee, J. B.; Chan, M. N.; Wu, Z.; Zuend, A.; Song, M. Viscosity and phase state of aerosol particles consisting of sucrose mixed with inorganic salts. *Atmos. Chem. Phys.* **2021**, *21*, 10215−10228.
(12) Huang, Y.; Mahrt, F.; Xu, S.; Shiraiwa, M.; Zuend, A.; Bertram, A. K. Coexistence of three liquid phases in individual atmospheric aerosol particles. *Proc. Natl. Acad. Sci. U.S.A.* **2021**, *118*, No. e2102512118.
(13) Jeong, R.; Lilek, J.; Zuend, A.; Xu, R.; Chan, M. N.; Kim, D.; Moon, H. G.; Song, M. Viscosity and physical state of sucrose mixed with ammonium sulfate droplets. *Atmos. Chem. Phys.* **2022**, *22*, 8805−8817.
(14) Kasparoglu, S.; Li, Y.; Shiraiwa, M.; Petters, M. D. Toward closure between predicted and observed particle viscosity over a wide range of temperatures and relative humidity. *Atmos. Chem. Phys.* **2021**, *21*, 1127−1141.
(15) Shiraiwa, M.; Seinfeld, J. H. Equilibration timescale of atmospheric secondary organic aerosol partitioning *Geophys. Res. Lett.* 2012, *39* 24, L24801 DOI: 10.1029/2012GL054008.
(16) Shiraiwa, M.; Pöschl, U. Mass accommodation and gas−particle partitioning in secondary organic aerosols: dependence on diffusivity, volatility, particle-phase reactions, and penetration depth. *Atmos. Chem. Phys.* **2021**, *21*, 1565−1580.
(17) Shiraiwa, M.; Yee, L. D.; Schilling, K. A.; Loza, C. L.; Craven, J. S.; Zuend, A.; Ziemann, P. J.; Seinfeld, J. H. Size distribution dynamics reveal particle-phase chemistry in organic aerosol formation. *Proc. Natl. Acad. Sci. U.S.A.* **2013**, *110*, 11746−11750.
(18) Zaveri, R. A.; Shilling, J. E.; Zelenyuk, A.; Liu, J.; Bell, D. M.; D'Ambro, E. L.; Gaston, C. J.; Thornton, J. A.; Laskin, A.; Lin, P.; et al. Growth kinetics and size distribution dynamics of viscous secondary organic aerosol. *Environ. Sci. Technol.* **2018**, *52*, 1191−1199.
(19) He, Y.; Akherati, A.; Nah, T.; Ng, N. L.; Garofalo, L. A.; Farmer, D. K.; Shiraiwa, M.; Zaveri, R. A.; Cappa, C. D.; Pierce, J. R.; Jathar, S. H. Particle size distribution dynamics can help constrain the phase state of secondary organic aerosol. *Environ. Sci. Technol.* **2021**, *55*, 1466−1476.

(20) Pajunoja, A.; Hu, W.; Leong, Y. J.; Taylor, N. F.; Miettinen, P.; Palm, B. B.; Mikkonen, S.; Collins, D. R.; Jimenez, J. L.; Virtanen, A. Phase state of ambient aerosol linked with water uptake and chemical aging in the southeastern US. *Atmos. Chem. Phys.* **2016**, *16*, 11163−11176.
(21) Bateman, A. P.; Gong, Z.; Liu, P.; Sato, B.; Cirino, G.; Zhang, Y.; Artaxo, P.; Bertram, A. K.; Manzi, A. O.; Rizzo, L. V.; et al. Sub-micrometre particulate matter is primarily in liquid form over Amazon rainforest. *Nat. Geosci.* **2016**, *9*, 34−37.
(22) Cheng, Z.; Sharma, N.; Tseng, K.-P.; Kovarik, L.; China, S. Direct observation and assessment of phase states of ambient and lab-generated sub-micron particles upon humidification. *RSC Adv.* **2021**, *11*, 15264−15272.
(23) Virtanen, A.; Joutsensaari, J.; Koop, T.; Kannosto, J.; Yli-Pirilä, P.; Leskinen, J.; Mäkelä, J. M.; Holopainen, J. K.; Pöschl, U.; Kulmala, M.; Worsnop, D. R.; Laaksonen, A. An amorphous solid state of biogenic secondary organic aerosol particles. *Nature* **2010**, *467*, 824−827.
(24) Liu, Y.; Wu, Z.; Huang, X.; Shen, H.; Bai, Y.; Qiao, K.; Meng, X.; Hu, W.; Tang, M.; He, L. Aerosol phase state and its link to chemical composition and liquid water content in a subtropical coastal megacity. *Environ. Sci. Technol.* **2019**, *53*, 5027−5033.
(25) Liu, Y.; Wu, Z.; Wang, Y.; Xiao, Y.; Gu, F.; Zheng, J.; Tan, T.; Shang, D.; Wu, Y.; Zeng, L.; et al. Submicrometer particles are in the liquid state during heavy haze episodes in the urban atmosphere of Beijing, China. *Environ. Sci. Technol. Lett.* **2017**, *4*, 427−432.
(26) Bateman, A. P.; Gong, Z.; Harder, T. H.; De Sá, S. S.; Wang, B.; Castillo, P.; China, S.; Liu, Y.; O'Brien, R. E.; Palm, B. B.; et al. Anthropogenic influences on the physical state of submicron particulate matter over a tropical forest. *Atmos. Chem. Phys.* **2017**, *17*, 1759−1773.
(27) Ministry of Environment. *2021: Annual Report of Air Quality in Korea, 2020*, NIER-GP2021-072, 2021; p 405.
(28) Ha, Y.; Kim, J.; Lee, S.; Cho, K.; Shin, J.; Kang, G.; Song, M.; Lee, J.; Jang, K. S.; Lee, K.; Ahn, J.; Wu, Z.; Matsuki, A.; Tang, N.; Sadanaga, Y.; Natsagdorj, A.; Kim, C. Spatiotemporal Differences on the Real-time Physicochemical Characteristics of PM2.5 Particles in Four Northeast Asian Countries During Winter and Summer 2020-2021.*Atmos. Res.* 2022, (in review).
(29) Ham, S.; Babar, Z. B.; Lee, J. B.; Lim, H.-J.; Song, M. Liquid−liquid phase separation in secondary organic aerosol particles produced from α-pinene ozonolysis and α-pinene photooxidation with/without ammonia. *Atmos. Chem. Phys.* **2019**, *19*, 9321−9331.
(30) Song, Y.-C.; Bé, A. G.; Martin, S. T.; Geiger, F. M.; Bertram, A. K.; Thomson, R. J.; Song, M. Liquid−liquid phase separation and morphologies in organic particles consisting of α-pinene and β-caryophyllene ozonolysis products and mixtures with commercially available organic compounds. *Atmos. Chem. Phys.* **2020**, *20*, 11263−11273.
(31) Kucinski, T. M.; Ott, E.-J. E.; Freedman, M. A. Dynamics of Liquid−Liquid Phase Separation in Submicrometer Aerosol. *J. Phys. Chem. A* **2021**, *125*, 4446−4453.
(32) Gaikwad, S.; Jeong, R.; Kim, D.; Lee, K.; Jang, K.-S.; Kim, C.; Song, M. Microscopic observation of a liquid-liquid-(semi) solid phase in polluted PM2.5. *Front. Environ. Sci.* **2022**, *10*, No. 1126.
(33) Renbaum-Wolff, L.; Grayson, J. W.; Bateman, A. P.; Kuwata, M.; Sellier, M.; Murray, B. J.; Shilling, J. E.; Martin, S. T.; Bertram, A. K. Viscosity of α-pinene secondary organic material and implications for particle growth and reactivity. *Proc. Natl. Acad. Sci. U.S.A.* **2013**, *110*, 8014−8019.
(34) Maclean, A. M.; Smith, N. R.; Li, Y.; Huang, Y.; Hettiyadura, A. P.; Crescenzo, G. V.; Shiraiwa, M.; Laskin, A.; Nizkorodov, S. A.; Bertram, A. K. Humidity-Dependent Viscosity of Secondary Organic Aerosol from Ozonolysis of β-Caryophyllene: Measurements, Predictions, and Implications. *ACS Earth Space Chem.* **2021**, *5*, 305−318.
(35) Maclean, A. M.; Li, Y.; Crescenzo, G. V.; Smith, N. R.; Karydis, V. A.; Tsimpidi, A. P.; Butenhoff, C. L.; Faiola, C. L.; Lelieveld, J.; Nizkorodov, S. A.; et al. Global Distribution of the Phase State and Mixing Times within Secondary Organic Aerosol Particles in the Troposphere Based on Room-Temperature Viscosity Measurements. *ACS Earth Space Chem.* **2021**, *5*, 3458−3473.
(36) Grayson, J. W.; Song, M.; Sellier, M.; Bertram, A. K. Validation of the poke-flow technique combined with simulations of fluid flow for determining viscosities in samples with small volumes and high viscosities. *Atmos. Meas. Tech.* **2015**, *8*, 2463−2472.
(37) Song, M.; Marcolli, C.; Krieger, U. K.; Zuend, A.; Peter, T. Liquid-liquid phase separation in aerosol particles: Dependence on O: C, organic functionalities, and compositional complexity *Geophys. Res. Lett.* 2012, *39* 19, L19801 DOI: 10.1029/2012GL052807.
(38) You, Y.; Smith, M. L.; Song, M.; Martin, S. T.; Bertram, A. K. Liquid−liquid phase separation in atmospherically relevant particles consisting of organic species and inorganic salts. *Int. Rev. Phys. Chem.* **2014**, *33*, 43−77.
(39) Ciobanu, V. G.; Marcolli, C.; Krieger, U. K.; Weers, U.; Peter, T. Liquid− liquid phase separation in mixed organic/inorganic aerosol particles. *J. Phys. Chem. A* **2009**, *113*, 10966−10978.
(40) Song, M.; Marcolli, C.; Krieger, U. K.; Lienhard, D. M.; Peter, T. Morphologies of mixed organic/inorganic/aqueous aerosol droplets. *Faraday Discuss.* **2013**, *165*, 289−316.
(41) Song, M.; Liu, P. F.; Hanna, S. J.; Zaveri, R. A.; Potter, K.; You, Y.; Martin, S. T.; Bertram, A. K. Relative humidity-dependent viscosity of secondary organic material from toluene photo-oxidation and possible implications for organic particulate matter over megacities. *Atmos. Chem. Phys.* **2016**, *16*, 8817−8830.
(42) Winston, P. W.; Bates, D. H. Saturated solutions for the control of humidity in biological research. *Ecology* **1960**, *41*, 232−237.
(43) Cummings, B. E.; Li, Y.; DeCarlo, P. F.; Shiraiwa, M.; Waring, M. S. Indoor aerosol water content and phase state in US residences: Impacts of relative humidity, aerosol mass and composition, and mechanical system operation. *Environ. Sci.: Processes Impacts* **2020**, *22*, 2031−2057.
(44) Lilek, J.; Zuend, A. A predictive viscosity model for aqueous electrolytes and mixed organic−inorganic aerosol phases. *Atmos. Chem. Phys.* **2022**, *22*, 3203−3233.
(45) Gkatzelis, G. I.; Papanastasiou, D. K.; Karydis, V. A.; Hohaus, T.; Liu, Y.; Schmitt, S. H.; Schlag, P.; Fuchs, H.; Novelli, A.; Chen, Q.; et al. Uptake of water-soluble gas-phase oxidation products drives organic particulate pollution in Beijing. *Geophys. Res. Lett.* **2021**, *48*, No. e2020GL091351.
(46) Petters, S. S.; Kreidenweis, S. M.; Grieshop, A. P.; Ziemann, P. J.; Petters, M. D. Temperature-and humidity-dependent phase states of secondary organic aerosols. *Geophys. Res. Lett.* **2019**, *46*, 1005−1013.
(47) Gervasi, N. R.; Topping, D. O.; Zuend, A. A predictive group-contribution model for the viscosity of aqueous organic aerosol. *Atmos. Chem. Phys.* **2020**, *20*, 2987−3008.
(48) Zaveri, R. A.; Shilling, J. E.; Zelenyuk, A.; Zawadowicz, M. A.; Suski, K.; China, S.; Bell, D. M.; Veghte, D.; Laskin, A. Particle-phase diffusion modulates partitioning of semivolatile organic compounds to aged secondary organic aerosol. *Environ. Sci. Technol.* **2020**, *54*, 2595−2605.
(49) Zaveri, R. A.; Wang, J.; Fan, J.; Zhang, Y.; Shilling, J. E.; Zelenyuk, A.; Mei, F.; Newsom, R.; Pekour, M.; Tomlinson, J.; et al. Rapid growth of anthropogenic organic nanoparticles greatly alters cloud life cycle in the Amazon rainforest. *Sci. Adv.* **2022**, *8*, No. eabj0329.
(50) Shiraiwa, M.; Garland, R. M.; Pöschl, U. Kinetic double-layer model of aerosol surface chemistry and gas-particle interactions (K2-SURF): Degradation of polycyclic aromatic hydrocarbons exposed to O_3, NO_2, H_2O, OH and NO_3. *Atmos. Chem. Phys.* **2009**, *9*, 9571−9586.
(51) Shiraiwa, M.; Ammann, M.; Koop, T.; Pöschl, U. Gas uptake and chemical aging of semisolid organic aerosol particles. *Proc. Natl. Acad. Sci. U.S.A.* **2011**, *108*, 11003−11008.
(52) Zaveri, R. A.; Easter, R. C.; Shilling, J. E.; Seinfeld, J. H. Modeling kinetic partitioning of secondary organic aerosol and size

distribution dynamics: representing effects of volatility, phase state, and particle-phase reaction. *Atmos. Chem. Phys.* **2014**, *14*, 5153−5181.

https://doi.org/10.1021/acs.est.2c06377
Environ. Sci. Technol. 2022, 56, 17581−17590